# Adsorption of hydrocarbons on a diamond (111) surface: An *ab initio* quantum-mechanical study

K. Larsson
*Institute of Chemistry, Uppsala University, Box 531, S-751 21 Uppsala, Sweden*

S. Lunell
*Department of Quantum Chemistry, Uppsala University, Box 518, S-751 20 Uppsala, Sweden*

J.-O. Carlsson
*Institute of Chemistry, Uppsala University, Box 531, S-751 21 Uppsala, Sweden*
(Received 16 October 1992; revised manuscript received 1 April 1993)

The adsorption of H·, $CH_3$·, $CH_2$, CH·, $C_2H$·, and $C_2H_2$ on hydrogen-terminated (111) surfaces of diamond has been investigated theoretically. *Ab initio* molecular-orbital theory was used in order to calculate the relative adsorption energies of these different hydrocarbon species. The effects of electron correlation, included by means of second-order Møller-Plesset theory, on the relative adsorption energies, as well as the choice of basis sets, were investigated. The effects of different sizes of model clusters and different geometry optimizations were also studied. Counterpoise corrections were used to estimate the magnitude of the basis-set superposition errors. The adsorption energies were found to be in the order $C_2H\cdot > H\cdot \approx CH_2(\text{singlet}) > CH\cdot > CH_2\cdot(\text{triplet}) > CH_3\cdot > C_2H_2$. The $C_2H$· species was predicted to adsorb stronger to the H-terminated diamond (111) surface than H· does. $C_2H_2$ with one site binding to the surface was predicted to yield a significantly weaker adsorption than the other hydrocarbons.

## I. INTRODUCTION

Within the last decade there has been a substantial increase in the interest of gas-phase synthesis of diamond under conditions where graphite is the thermodynamically most stable form of carbon. This interest is mostly due to the exceptional properties of diamond (e.g., extreme hardness, high thermal conductivity and electric resistivity, optical transparency, chemical inertness). The development of the low-pressure synthesis will open up new fields for applications. These include fabrication of wear-resistant protective coatings, abrasives, heat sinks, and high-temperature semiconducting and optical devices. However, the realization of these applications will be determined by the degree of success in the well-controlled growth of diamond of high crystal quality. It is therefore of highest importance to achieve a detailed understanding of the nucleation and growth process at the molecular level.

In spite of considerable effort, much of the underlying chemical and physical growth mechanisms remain uncertain. The first attempts in the direction of achieving knowledge about the molecular level surface chemistry were based on semiempirical quantum chemical calculations. Tsuda, Nakajima, and Oikawa[1,2] and Frenklach and co-workers[3,4] proposed different growth mechanisms for the diamond (111) surface. In the work of Tsuda, Nakajima, and Oikawa,[1,2] the growth mechanism was based on methyl addition. The acetylene molecule was proposed as the primary growth species by Frenklach and co-workers.[3,4] Huang and Frenklach have also studied the energetics of methyl-followed-by-acetylene addition.[5] The energetically most favorable reaction path led to the formation of stacking faults and structural defects.

Growth of diamond requires adsorption of a hydrocarbon species (the growth species) to a surface site on the hydrogenated diamond surface. It is therefore of great interest to investigate more systematically the adsorption of different hydrocarbon species on a diamond surface. Recently, different theoretical methods have been used to investigate the adsorption energy of a variety of hydrocarbon species adsorbed on the diamond (111) surface (see Sec. III F). Semiempirical methods, used by Valone, Trkula, and Laia[7] and Mehandru and Andersson,[6] have yielded disparate results. More recently, Pederson, Jackson, and Picket[8,9] and Mintmire *et al.*[10] have used local-density approximations in order to calculate the energy of adsorption of not only different hydrocarbon species, but also of hydrogen, on the diamond (111) surface. Their ordering of hydrogen and hydrocarbon species on the energy scale is different from the result of Brenner[11] who used an empirical potential-energy function in calculating the adsorption energies of these species.

The purpose of the present paper is to investigate the adsorption of various species on a hydrogenated diamond (111) surface using *ab initio* molecular-orbital theory. The gaseous species which have been used in the calculations are H·, $CH_3$·, $CH_2$, CH·, $C_2H$·, and $C_2H_2$. All of them may be formed in the gas phase during diamond deposition. The major part of the present work is a methodological study in which the effects of different factors on the calculated relative adsorption energies have been investigated systematically. These factors include the effects of different sizes of basis sets and of the templates modeling the cluster to which the adsorbate is bound, as well as electron correlation corrections.

A necessary condition for obtaining a good description of the electronic state of the reactants and products in the

0163-1829/93/48(4)/2666(9)/$06.00  

adsorption reaction is primarily to choose a highly flexible basis set, a model cluster (template) describing the diamond surface well, and to use treatments which include electron correlation. Geometry optimizations are also of vital importance. In practice, however, it is not possible to use a large improvement of the basis sets together with a large improvement of the correlation technique for the template sizes used in this work. As a preparation for further work, it is therefore necessary to make a methodological study in which the effect of these choices on the relative adsorption energies are investigated.

## II. METHOD

The adsorption of different species to a radical carbon atom on a hydrogenated diamond (111) surface has been investigated theoretically within *ab initio* molecular-orbital theory, using the program system GAUSSIAN90.[12] The adsorbed species are the five hydrocarbons $CH_3\cdot$, $CH_2$, $CH\cdot$, $C_2H\cdot$, and $C_2H_2$ and hydrogen $H\cdot$. Thermodynamic calculations have shown that these hydrocarbons are present at equilibrium in the gas phase during diamond deposition in hot filament and plasma chemical vapor deposition (CVD) reactors.[13] The single bond that forms between the radical species and the surface results from $\sigma$ overlap between the surface dangling orbital and a corresponding orbital of the adsorbate.

The $CH_2$ species can be found in two different low-lying electronic states, one singlet state ($^1A_1$) and one triplet state ($^3B_1$). The triplet state is predicted to be more stable by approximately 140 kJ/mol.[14] The present calculations consider both electronic states. A onefold site adsorption of $C_2H_2$ is assumed, i.e., $C_2H_2$ binds to the surface radical carbon through one end. This bonding is illustrated in a correlation diagram in Ref. 6. The $\pi$ and $\pi^*$ orbitals in $C_2H_2$ mix in such a way that a localized $\sigma$ bond between $C_2H_2$ and the surface radical carbon is formed.

The present work includes calculations of the total electronic energies for the reactants as well as for the products of the adsorption,

$$M\cdot + C_XH_Y\cdot \rightarrow M\text{-}C_XH_Y \ , \tag{1}$$

where $M$ is the model cluster. The relative adsorption energies were then calculated by using

$$\begin{aligned}\Delta E_{\mathrm{rel},C_xH_y\cdot} &= E_{\mathrm{ads},C_xH_y\cdot} - E_{\mathrm{ads},H\cdot} \\ &= E_{C_xH_y\cdot} + E_{M\text{-}H\cdot} - E_{H\cdot} - E_{M\text{-}C_xH_y\cdot} \ .\end{aligned} \tag{2}$$

$E_{\mathrm{ads},C_xH_y\cdot}$ and $E_{\mathrm{ads},H\cdot}$ are the adsorption energies for the different species $C_xH_y\cdot$ and $H\cdot$. $E_{C_xH_y\cdot}$, $E_{M\text{-}H}$, $E_{H\cdot}$, and $E_{M\text{-}C_xH_y}$ are the total electronic energies for the different gaseous species and for the template $M$ with an adsorbed species, respectively.

A complication in these calculations is that the basis functions located on the template atoms partly overlap the adsorbed molecules, and vice versa. This will lead to an artificial lowering of the energies of both the adsorbate and the template, separate from the pure binding effects. The effect of this "basis-set superposition error" (BSSE) (Ref. 15) is, hence, that the calculated adsorption energies will be too large. To estimate the magnitude of BSSE, additional calculations were carried out, where the complete basis sets of the "supermolecule" (template+adsorbate) were used also to compute the energies of the separate adsorbate and template, respectively. The corrections to the total energies obtained in this way, commonly called "counterpoise corrections,"[15] were then subtracted from the total binding energy.

The radical and nonradical reactants and products in the adsorption expression were described by spin unrestricted and restricted Hartree-Fock wave functions, respectively. The simplest level of *ab initio* molecular-orbital theory involves the use of a minimal basis set of atomic functions. However, since a minimal basis set contains only a single valence function of each particular symmetry type (e.g., $s,p,d$), such effects as expansion or contraction of the electron distribution around a particular atom in response to differing molecular environments, which accompany the formation of a chemical bond are not well described by such a basis. For this reason most of the present calculations use split-valence basis sets, with or without polarization functions. The split-valence basis set is an extension of the minimal basis set, in which the basis functions representing the valence electrons are doubled. However, these basis sets are still centered at nuclear positions. An improved description of the charge rearrangement occurring around the atoms, especially angular redistributions, is obtained by adding polarization functions ($p$ to H and $d$ to C) to the split-valence basis set.

All geometrical parameters for the six adsorbate species investigated were fully optimized. For the template, with or without an adsorbed species, only the radical carbon atom of the template was allowed to relax in the field of a fixed structure of its neighbors. As a check, the three nearest neighbors to the central carbon on the template were also allowed to relax in a Hartree-Fock energy calculation of the adsorption of hydrogen. No change in adsorption energy was then observed. The geometries of the adsorbed species on the hydrogenated diamond (111) surface are presented in Table I.

## III. RESULTS AND DISCUSSION

### A. Influence of template sizes

Three different diamond templates, representing a (111) surface, have been used to study the influence of the size of the template on the adsorption energy. The largest diamond template consists of a four-layer-thick $C_{22}H_{27}\cdot$ template (Fig. 1). The framework of this template consists of a central atom (the radical carbon), the nearest three carbon atoms, and the next-nearest nine carbon atoms. Hydrogen atoms, together with nine additional hydrogen-terminated carbon atoms, terminate the cluster. A terminated C-H distance of 1.1 Å was used. Six of the next-nearest neighbors to the surface radical carbon are also surface carbons, which might adsorb species that may induce steric hindrances. The missing bond to the

TABLE I. Geometry of adsorbed species.

| | $CH_3\cdot$ | $CH_2$ | $CH\cdot$ | $C_2H\cdot$ | $C_2H_2$ |
|---|---|---|---|---|---|
| $r_{C\text{-}C}$[a] (Å) | 1.563 | 1.524 | 1.502 | 1.487 | 1.557 |
| $r_{C\text{-}C}$ (Å) | | | | 1.189 | 1.329 |
| $r_{C\text{-}H}$ (Å) | 1.077 | 1.070 | 1.064 | 1.057 | 1.071[b] |
| | | | | | 1.068[c] |
| $\alpha_{C\text{-}C\text{-}H}$[a] (deg) | 112.8 | 122.3 | 180.0 | 180.0 | 113.4 |
| $\alpha_{H\text{-}C\text{-}H}$ (deg) | 55.2 | 60.2 | | | 110.3[d] |
| | | | | | 140.3[e] |

[a]Radical carbon on the diamond surface.
[b]Distance between the binding carbon (I) on the adsorbed species and its neighboring hydrogen (I).
[c]Distance between the carbon (II) on the adsorbed species and its neighboring hydrogen (II).
[d]$\alpha_{H(I)\text{-}C(I)\text{-}C(II)\cdot}$
[e]$\alpha_{C(I)\text{-}C(II)\text{-}H(II)\cdot}$

radical carbon yields a singly occupied *sp*-hybridized dangling orbital. Table II shows the dependence of the relative adsorption energies on the template size. The adsorption energies for the different species are given relative to the adsorption energy of $H\cdot$.

One of the smallest templates that has been used in the literature to describe the diamond (111) surface is a two-layer-thick $C_4H_9\cdot$ template (Fig. 2).[16] It has been assumed that this small hydrocarbon template, with a tertiary carbon atom, can be used in the calculation of activation energies for surface abstraction reactions in diamond growth. In comparison with an unconstrained $C_4H_9\cdot$ template, an increase in the abstraction energy of only 0.8 kJ/mol was calculated for the tertiary carbon atom constrained in the same way as in diamond. Since the use of as small a template as possible is a clear computational advantage, it was of interest to investigate the possibility of obtaining reliable relative adsorption energies when performing calculations based on this small template. The carbon framework of this model is only the central carbon atom and its three nearest carbon neighbors. These three carbon atoms are terminated with hydrogens at a distance of 1.10 Å. The dangling bond of the surface radical carbon, hence, has no hydrogen neighbors. This will result in an elimination of repulsions that otherwise take place between the incoming gaseous species and the hydrogens (steric effects).

The results of calculations based on this small template are given in Table II. The ordering of the relative adsorption energies is identical to the corresponding ordering obtained by performing calculations based on the largest template $C_{22}H_{27}\cdot$. However, the steric effects due to the existence of neighboring hydrogen atoms to the radical carbon are evident when comparing the results from calculations based on the $C_{22}H_{27}\cdot$ and $C_4H_9\cdot$ templates, respectively. This is especially the case for the

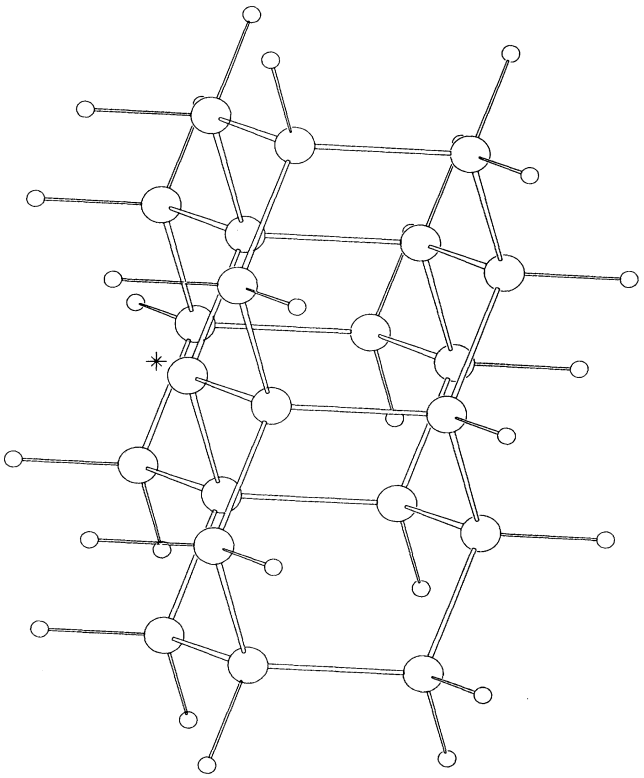

FIG. 1. The template $C_{22}H_{27}\cdot$. The larger circles designate carbon atoms, and the smaller circles designate hydrogen atoms. The marked atom is the radical surface carbon on which the different hydrocarbon species are adsorbed.

TABLE II. Effect of cluster size on relative adsorption energies. Values in parentheses are the adsorption energies $\Delta E_H$. Calculations were performed at the Hartree-Fock (3-21*G*/STO-3*G*) level (kJ $mol^{-1}$).

| $\Delta E_x - \Delta E_H$ | $C_{22}H_{27}\cdot$ | $C_{13}H_{21}\cdot$ | $C_4H_9\cdot$ |
|---|---|---|---|
| $CH_2$(singlet) | 37 | 39 | 68 |
| $C_2H$ | 33 | 33 | 37 |
| $H\cdot$ | 0(382) | 0(386) | 0(364) |
| $CH\cdot$ | −48 | −47 | −41 |
| $CH_2\cdot$(triplet) | −105 | −103 | −75 |
| $CH_3\cdot$ | −140 | −137 | −81 |
| $C_2H_2$ | −312 | −310 | −246 |

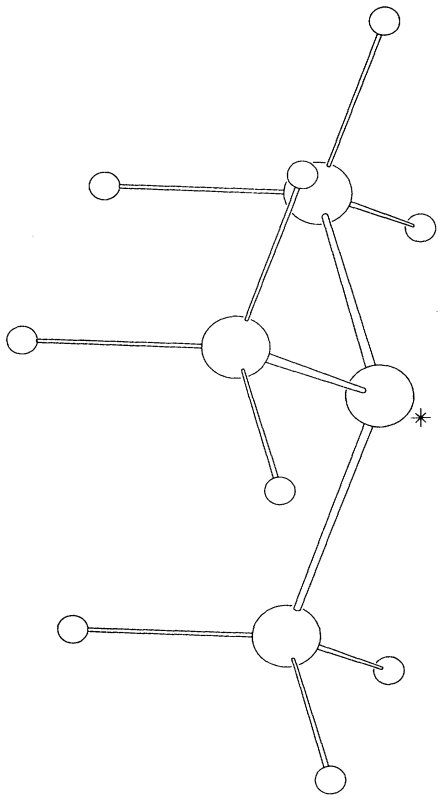

FIG. 2. The template $C_4H_9\cdot$. Symbols as in Fig. 1.

nonlinear species, e.g., $CH_3\cdot$, $CH_2$ (singlet), $CH_2\cdot$ (triplet), and $C_2H_2$. The relative adsorption energies for these species have increased by at least 30 kJ/mol when removing the steric effect of neighboring hydrogens by choosing the smaller template $C_4H_9\cdot$ in the adsorption energy calculations.

These results eliminate the template $C_4H_9\cdot$ to usefully model the diamond (111) surface in adsorption reaction calculations. The main reason for that is the steric effects. As can be seen in Table II, these effects for the $CH_3\cdot$, $CH_2$(singlet), $CH_2\cdot$(triplet), and $C_2H_2$ species are 59, 31, 30, and 66 kJ/mol, respectively, when comparing the results of calculations based on the $C_{22}H_{27}\cdot$ and $C_4H_9\cdot$ templates. These effects are unacceptably large. For this reason, an intermediate-sized template was sought, which would reproduce the essential features of the larger $C_{22}H_{27}\cdot$ template. A diamond (111) surface model with 13 carbon atoms ($C_{13}H_{21}\cdot$) was chosen. The number of carbon atoms in this model is nine more than in $C_4H_9\cdot$ but nine less than in $C_{22}H_{27}\cdot$, the largest template. Compared to the largest template, this reduction makes it possible to consider electron correlation in the calculations. It is also possible to use a more flexible basis set with this medium-sized $C_{13}H_{21}\cdot$ template, compared with the largest $C_{22}H_{27}\cdot$ template.

The framework of $C_{13}H_{21}\cdot$ differs mainly from that for the largest template $C_{22}H_{27}\cdot$ in that the next-nearest neighbors to the central radical carbon consists of six carbon atoms and three hydrogen atoms (Fig. 3), as compared to nine next-nearest carbon atoms in $C_{22}H_{27}\cdot$. This difference in the type of neighbors results in a two-layer-thick carbon template with six hydrogenated carbon neighbors to the surface radical carbon atom. The carbon atoms in this template are also terminated by hydrogen atoms at a distance of 1.10 Å.

The effect of using this medium-sized template in the calculations can also be seen in Table II. The relative energy values for the different adsorbing species are compared with the corresponding ones when using the largest template $C_{22}H_{27}\cdot$ in the calculations. The largest energy difference for the two template sizes is 3 kJ/mol, which is found for the adsorption of the $CH_3\cdot$ group. The relative adsorption energy is $-140$ kJ/mol when using the largest template, which is compared with the relative adsorption energy of $-137$ kJ/mol for $C_{13}H_{21}\cdot$. This energy difference is small compared to the obtained differences within each group of adsorption energies (one group defined as belonging to the $C_{13}H_{21}\cdot$ template and the other to the $C_{22}H_{27}\cdot$ template). The correction for BSSE (see Sec. III D) does not alter this conclusion. Thus it is concluded that the $C_{13}H_{21}\cdot$ template is adequate to use in the further study of the adsorption reactions.

When a hydrogen atom is removed from the hydrogenated diamond (111) surface, the central carbon atom changes its hybridization from $sp^3$ towards $sp^2$. The radical carbon atom then sinks down into the fixed frame-

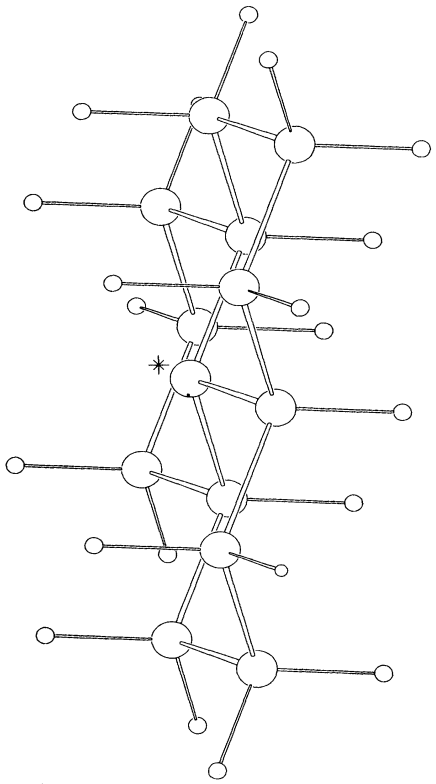

FIG. 3. The template $C_{13}H_{21}\cdot$. Symbols as in Fig. 1.

work of the neighboring carbon atoms. The magnitude of this vertical relaxation was calculated to be 0.12 Å for the $C_4H_9\cdot$ cluster, 0.15 Å for the $C_{13}H_{21}\cdot$ cluster, and 0.11 Å for the $C_{22}H_{27}\cdot$ cluster. These values are somewhat smaller, but qualitatively similar to those obtained by Jackson,[17] using a method based on the local-density approximation. For similar clusters, $C_4H_9\cdot$, $C_{13}H_{21}\cdot$, and $C_{22}H_{27}\cdot$, Jackson reports the values 0.17, 0.18, and 0.16 Å, respectively. Both sets of calculations thus support a partial transition to $sp^2$ hybridization at the radical site. The local geometry is, however, still quite far from a completely planar, $sp^2$ hybridized one, which is consistent with the notion that one electron remains in the dangling-bond orbital.

### B. Influence of basis sets

The effect of different basis sets on the relative adsorption energies was investigated systematically. These calculations were based on the $C_{13}H_{21}\cdot$ template in modeling the hydrogenated diamond (111) surface. The basis sets that were examined are the approximate Slater-type orbitals (STO-3G) minimal basis set and the split-valence basis sets 3-21*G*, 6-31*G*, and 6-31*G***.[18] The STO-3G basis set is a minimal basis set where each atomic orbital (AO) is expanded in terms of three Gaussian functions. In the 3-21*G* and 6-31*G* bases, the valence AO's are expanded in terms of two contracted basis functions, constructed from two and one primitive Gaussians, respectively, in the case of 3-21*G*, and three and one primitive Gaussians, respectively, in the case of 6-31*G*. The inner-shell atomic orbitals are represented by single basis functions, which are contractions of three (3-21*G*) or six (6-31*G*) primitive Gaussians. As mentioned above, these split-valence basis sets are able to give an improved description of expansion or contraction of the valence shell in response to differing molecular environments.

The polarized basis set 6-31*G** is constructed by adding a set of *d*-type primitive Gaussians to the split-valence 6-31*G* basis set for nonhydrogen atoms. However, a possible polarization of the *s* orbitals on the hydrogen atoms, especially those closest to the adsorption site, must also be allowed. The more complete basis set, 6-31*G***, which in addition contains a single set of Gaussian *p*-type functions on each hydrogen, was therefore used.

A combination of two different basis sets was used for the $C_{13}H_{21}\cdot$ template. The radical carbon atom and its three nearest carbon neighbors were represented by a basis set called *A*, while the remaining atoms were represented by a slightly smaller basis set called *B*. The gaseous and adsorbed species were all represented by *A*. This division is due to practical considerations. The calculation would be very time consuming if calculations were performed using, e.g., the 6-31*G*** representation for all atoms in the system. Hence, a division of basis sets has been used in the calculations, where the more flexible basis set is used near the region of adsorption.

The three combinations of basis sets included in the comparison are 3-21*G*/STO-3*G*, 6-31*G***/STO-3*G*, and 6-31*G***/6-31*G*. Table III shows the effect of the basis set on the relative adsorption energies calculated at the Hartree-Fock level. The results show that the relative adsorption energies are rather similar for the two different basis set combination 3-21*G*/STO-3*G* and 6-31*G***/STO-3*G*. Thus, the effect on the relative adsorption energies of adding polarization functions on the atoms in group *A*, without improving the *B* basis, is small. There is a larger difference between the relative adsorption energies calculated by using the 6-31*G***/6-31*G* combination compared to the corresponding energies calculated by using the 6-31*G***/STO-3*G* combination. This shows that the effects of the adsorption on the next-nearest neighbors are not satisfactorily described by using the STO-3*G* basis set for the latter.

TABLE III. Effect of basis size on relative adsorption energies. $\Delta E_x - \Delta E_H$ / (kJ mol$^{-1}$).

| | 3-21*G*/STO-3*G* | 6-31*G***/STO-3*G* | 6-31*G***/6-31*G* |
|---|---|---|---|
| $CH_2$(singlet) | 39 | 38 | 26 |
| $C_2H\cdot$ | 33 | 39 | 22 |
| $H\cdot$ | 0 | 0 | 0 |
| $CH\cdot$ | −47 | −48 | −60 |
| $CH_2\cdot$(triplet) | −103 | −92 | −104 |
| $CH_3\cdot$ | −137 | −131 | −145 |
| $C_2H_2$ | −310 | −295 | −308 |

Numerically, the differences in relative adsorption energies between different combinations of basis sets are, from Table III, seen to be in some cases larger than the differences in relative adsorption energies within a given combination of basis sets. Nevertheless, the ordering of the relative adsorption energies is, with one exception, the same for the three different combinations of basis sets. It is only the $CH_2$ (singlet) and $C_2H\cdot$ groups that exchange their relative positions on the energy scale in one of the calculations, namely that using the 6-31*G***/STO-3*G* basis-set combination. The energy difference is, however, in this case less than 2 kJ/mol. As will be seen in the next section, this energy difference is negligible in comparison with the difference in correlation energy between the two species.

The ordering of the relative adsorption energies for all species is the same for the three different combinations of basis sets when counterpoise corrections are included (see Sec. III D).

### C. Influence of electron correlation

The primary deficiency of Hartree-Fock theory is the inadequate treatment of the instantaneous correlation between motions of electrons. It is well known that the main part of the correlation energy comes from electrons with opposite spins, since electrons with parallel spins are automatically kept apart because of the antisymmetry of the wave function (the so-called "Fermi hole"). A crude but commonly used estimate is that the correlation energy is approximately 1 eV/electron pair. These effects are, hence, of special importance if new bonds are formed between atoms. Calculation of the adsorption energies on

the Hartree-Fock level gives then rather poor results since the adsorption reactions in the present cases generally result in a new pairing of electrons.

The calculated energies for dissociation of different $AB$ compounds have been compared with experimental values in Ref. 18, where both $A$ and $B$ are hydrides of the first period elements. These energy values are also relevant for adsorption reactions since the latter types of reactions are the reverse of the dissociation of bonds. The "adsorption" of various first row hydrides ($B$) to a methyl group ($A$) is of special interest for our investigation since the methyl group is closely related to the diamond template models in the present work. The results given in Ref. 18 show that Hartree-Fock (6-31$G^{**}$ basis set) energies, in general, are in very poor agreement with experiment, being typically in error by 108–188 kJ/mol. The theoretical results improve substantially when performing electron correlation treatments using second-order Møller-Plesset perturbation theory (MP2). The bond-dissociation energies are then in error by less than 8 kJ/mol at the MP2/6-31$G^{**}$ level.[18] This accuracy should be sufficient for the calculations of the adsorption energies in the present work.

The results of MP2 calculations for the adsorption of the different gaseous species on the hydrogenated diamond (111) surface are given in Table IV. The $C_{13}H_{21}$· template is used to model the diamond surface. No geometry optimization was performed in the electron correlation calculations. Instead, the optimized geometry obtained at the Hartree-Fock level was used. The results of the electron correlation treatment based on the 6-31$G^{**}$/STO-3$G$ combination of basis sets (see Sec. III B) are very interesting. It is only the $CH_2$·(triplet) and CH· groups that exchange their relative position on the energy scale. Their relative adsorption energies have changed from −92 and −48 kJ/mol, respectively, to −25 and −41 kJ/mol, respectively. The difference between the relative adsorption energies for $CH_2$(singlet) and for $C_2H$· is now very large, about 120 kJ/mol. Furthermore, the difference between the relative adsorption energies for $CH_3$· and for CH has decreased from 83 to 12 kJ/mol. The ordering of the different species on the adsorption energy scale is now $C_2H$· > $CH_2$(singlet) > H· > $CH_2$·(triplet) > CH > $CH_3$·$C_2H_2$.

The deficiency of the Hartree-Fock method is also shown in Table V, where the absolute adsorption energies for the different gaseous species are shown. They are obtained from calculations on the Hartree-Fock and MP2 levels, respectively, using the 6-31$G^{**}$/STO-3$G$ basis-set combination. As expected, the changes obtained when performing the calculations with electron correlation included are large, 8–247 kJ/mol.

The smallest values of the electron correlation corrections for the hydrocarbon species are related to the adsorption of $CH_2$(singlet) and $C_2H_2$ (8 and 25 kJ/mol, respectively). It is quite understandable that the adsorption of these species to the diamond (111) surface leads to the smallest electron correlation corrections since no new pairing of electrons is expected during the adsorption reactions.

The largest electron correlation correction (247 kJ/mol) is related to the adsorption of $C_2H$·. In this species there is a short triple bond and the bond length will be shortened additionally during the adsorption reaction ($\Delta r_{C\text{-}C}=0.026$ Å). The $C_2H$· group has also the shortest C-C bond (1.487 Å) to the radical carbon atom on the diamond (111) surface. The rather large value of the electron correlation correction can then in part be explained as an effect of the shortened triple bond, and in part be explained as an effect of the very short carbon bond to the diamond surface and the resulting high electron density in the binding region.

It would be interesting to make MP2 correlation treatments in conjunction to the more flexible basis-set combination 6-31$G^{**}$/6-31$G$. However, this becomes too expensive as the number of functions in the basis set are increased. One way to overcome this problem and to obtain approximate correlated relative energies is to assume additivity of correlation and basis-set enhancement effects.[18] One then assumes that the effect on the relative energies by using 6-31$G^{**}$/6-31$G$ instead of 6-31$G^{**}$/STO-3$G$, is the same at the Hartree-Fock and MP2 levels.

The estimated effects of adding the electron correlation corrections to the result of the 6-31$G^{**}$/6-31$G$ basis set for each species are shown in Table IV. The ordering of

TABLE IV. Effect of electron correlation on relative adsorption energies. $\Delta E_x - \Delta E_H$ (kJ mol$^{-1}$).

| | HF (6-31$G^{**}$/STO-3$G$) | MP2 (6-31$G^{**}$ /STO-3$G$) | HF (6-31$G^{**}$/6-31$G$) | MP2[a] (6-31$G^{**}$/6-31$G$) |
|---|---|---|---|---|
| $C_2H$· | 39 | 187 | 22 | 170 |
| $CH_2$(singlet) | 38 | 62 | 26 | 50 |
| H· | 0 | 0 | 0 | 0 |
| CH· | −48 | −41 | −60 | −53 |
| $CH_2$·(triplet) | −92 | −25 | −104 | −37 |
| $CH_3$· | −131 | −53 | −145 | −67 |
| $C_2H_2$ | −295 | −369 | −308 | −382 |

[a]Estimated from the expression:

$$\Delta E[\text{MP2/(6-31}G^{**}\text{/6-31}G)] = \Delta E[\text{MP2/(6-31}G^{**}\text{/STO-3}G)] + \Delta E[\text{HF/(6-31}G^{**}\text{/6-31}G)] - \Delta E[\text{HF/(6-31}G^{**}\text{/STO-3}G)] .$$

TABLE V. Binding energies for adsorbed hydrocarbon species on a $C_{13}H_{21}$· cluster, calculated at different levels of approximation (numbers within parentheses include BSSE corrections).

| $\Delta E_{ads}$ (kJ mol$^{-1}$) | HF[a] | HF[b] | MP2[a] |
|---|---|---|---|
| $C_2H$· | 411 | 390 (377) | 658 (586) |
| $CH_2$(singlet) | 410 | 394 (372) | 418 (451) |
| H· | 372 | 368 (364) | 471 (454) |
| CH· | 324 | 308 (299) | 430 (378) |
| $CH_2$·(triplet) | 280 | 264 (242) | 446 (364) |
| $CH_3$· | 241 | 223 (211) | 418 (345) |
| $C_2H_2$ | 77 | 60 (48) | 102 (26) |

[a]6-31$G$**/STO-3$G$.
[b]6-31$G$**/6-31$G$.

the relative adsorption energies of the different species is identical to the corresponding MP2 ordering based on the less flexible 6-31$G$**/STO-3$G$ basis set. Hence, the limitations of this basis set does not influence the ordering of hydrogen and hydrocarbon species on the energy scale, since the basis-set effects are significantly smaller than the electron correlation corrections, as already mentioned.

### D. Basis-set superposition effects

Corrections for BSSE are made for the adsorption of the different gaseous species on the hydrogenated diamond (111) surface at the HF/(6-31$G$**/6-31$G$) and MP2/(6-31$G$**/STO-3$G$) levels of theory (Table V). The $C_{13}H_{21}$· template is used to model the diamond surface.

As can be seen in Table V, the BSSE for hydrogen H· is 4 and 17 kJ/mol at the HF/(6-31$G$**/6-31$G$) and MP2/(6-31$G$**/STO-3$G$) levels of theory, respectively. The corresponding ranges of BSSE for the hydrocarbons are 9–22 and 52–82 kJ/mol. The BSSE's calculated at the Hartree-Fock level are, with one exception, too small to change the ordering of the relative adsorption energies. It is only the $CH_2$(singlet) and $C_2H$· groups that exchange their relative position on the energy scale. This reflects that the HF adsorption energies are very similar for these species. However, the BSSE's at the MP2 level of theory are larger and will consequently influence the ordering of the relative adsorption energies more. The $CH_2$(singlet) and H· groups, as well as the $CH_2$·(triplet) and CH· groups, have exchanged their positions on the energy scale. The corrections for BSSE have resulted in adsorption energies that are very similar especially for the $CH_2$(singlet) and H· groups, with an energy difference of only 4 kJ/mol (adsorption energies 451 and 454 kJ/mol, respectively). The ordering of the different species on the adsorption energy scale is now the following: $C_2H$· > H· ≈ $CH_2$(singlet) > CH· > $CH_2$·(triplet) > $CH_3$· > $C_2H_2$.

### E. Adsorption energies in relation to diamond growth

In this work, the adsorption energies were calculated under the assumption of a rigid structure (no vibrations included). It is then rather difficult to draw more thorough conclusions regarding the adsorption on the diamond surface, since these type of reactions occur at a high temperature (~1300 K). Knowledge of the complicated high-temperature dynamics is then required. Nevertheless, the result of these calculations can be regarded as a hint when trying to understand the experimental results.

Earlier experimental studies of diamond growth mechanisms on the (111), (100), and (110) crystal faces of natural diamond have been performed by Chu *et al.*[19] Competition studies by using carbon-13-labeled methane and carbon-12 acetylene were made. The carbon-13 mole fraction of the diamond film indicated that the methyl radical is the dominant growth species under the hot-filament CVD conditions for the (111) and (100) orientations of the diamond substrate. The fastest homepitaxial growth rate of 1.3 $\mu$m/h was obtained for growth on the (110) surface. It was not clear if methyl radicals would be the primary growth species on an ideal (110) surface.

In the work by Geiss *et al.*[20] it was also shown that the fastest growing face of diamond under typical CVD conditions was (110). Belton and Harris[21] have proposed a detailed deposition mechanism involving addition of $C_2H_2$ to a (110) diamond surface. With this mechanism a good agreement between calculated and observed growth rates was obtained.

The calculated adsorption energy of the gaseous species $CH_3$· on the hydrogenated diamond (111) surface was predicted in the present work to be much larger than the adsorption energy for the onefold adsorption of $C_2H_2$ (345 compared to 26 kJ/mol, cf. Table V).

During filament-assisted diamond deposition from a reaction mixture of methane and hydrogen there is a mixture of $CH_3$· and $C_2H_2$ present in the gas phase above the substrate surface. The concentrations of each of these two species must be estimated before any conclusions can be drawn regarding the dominant growth species. This has been done in different *in situ* experiments.[22–24] The $C_2H_2$ concentration was estimated to be almost equal to the $CH_3$· concentration. Kinetic modeling showed that the concentration of $CH_2$ and $C_2H$· is much lower than the concentrations of $CH_3$· and $C_2H_2$ (by about two and four orders of magnitude, respectively).

The significant difference in adsorption energy between

$CH_3\cdot$ and $C_2H_2$, together with the fact that the gas-phase concentrations of these species are about the same, will then support a diamond growth on the diamond (111) surface based on the $CH_3\cdot$ group as a dominant growth species during filament-assisted diamond deposition from a reaction mixture of methane and hydrogen. Hence, this result is consistent with the experimental results of Chu *et al.*[19]

The calculated adsorption energies of the species $CH\cdot$, $CH_2$(singlet), $CH_2\cdot$(triplet), and $C_2H\cdot$ were also found to be larger than the adsorption energy of the $CH_3\cdot$ group in the present work (Table IV). However, the effect of these high adsorption energies on diamond growth is counteracted by the effect of the low gas-phase concentrations. The species $C_2H\cdot$ has the largest adsorption energy, but the concentration in the gas phase is estimated to be about four orders of magnitude less than the concentrations of the gaseous species $CH_3\cdot$ and $C_2H_2$.[22] We believe that this very low concentration precludes $C_2H\cdot$ from a significant role as a growth species on the diamond (111) surface. Calculations to examine relative adsorption energies of hydrogen and different hydrocarbons on the diamond (110) and (100) surfaces are under way.

### F. Comparison with previous calculations

The adsorption and bonding of $CH_3\cdot$, $CH_2$(singlet), $CH\cdot$, $C_2H\cdot$, and $C_2H_2$ to hydrogenated diamond (111) surfaces were investigated in the framework of the atom superposition and electron delocalization molecular-orbital method by Mehandru and Andersson.[6] The adsorption energies were estimated to be in the following order: $C_2H\cdot > CH\cdot \approx CH_2(\text{singlet}) > CH_3\cdot$. The onefold adsorption of $C_2H_2$ to a H-covered surface was predicted to be unstable.

The coverage dependence of the heat of formation for submonolayers of $CH_3\cdot$ and $C_2H\cdot$ groups coadsorbed with H on a diamond (111) surface was examined numerically with the AM1 semiempirical molecular-orbital method in the work by Valone, Trkula, and Laia.[7] They found that the addition of $CH_3\cdot$ groups is energetically favored over addition of $C_2H\cdot$ groups at lower coverages. This result is obviously contradictory to the result of Mehandru and Andersson.[6]

The energies of adsorption of not only different hydrocarbon species, but also of hydrogen H, on the diamond (111) surface, were investigated by using an empirical many-body potential-energy expression developed by Brenner.[11] The adsorption energies were predicted to be in the following order: $H\cdot > C_2H\cdot > CH_3\cdot$. Pederson, Jackson, and Picket[8,9] and Mintmire *et al.*[10] have also simulated interactions between the diamond (111) surface and hydrogen and hydrocarbons, respectively, by using the local-density approximation (LDA). The resulting ordering of the species $H\cdot$, $CH_3\cdot$, $C_2H\cdot$, and $C_2H_2$ on the adsorption energy scale was found to be $C_2H\cdot > H\cdot > CH_3\cdot > C_2H_2$ (onefold adsorption) in both the work by Pederson, Jackson, and Picket,[8,9] and in the work by Mintmire *et al.*[10] This result is not in agreement with the work by Brenner.[11] However, the differences in adsorption energies calculated by Brenner[11] are smaller than about 20 kJ/mol, which makes the ordering of species on the energy scale rather unreliable.

The present work results in an order of adsorption energies which is in agreement with the work by Pederson, Jackson, and Picket[8,9] and Mintmire *et al.*[10] A quantitative comparison of the adsorption energies shows very good agreement between the present MP2 results for $C_2H\cdot$, $H\cdot$, $CH_3\cdot$, and $C_2H_2$ (658, 471, 418, and 102 kJ/mol, respectively, see Table V) and the LDA results 637, 473, 434, and 164 kJ/mol, reported by Pederson, Jackson, and Picket[8,9] or the values 578, 405, 415, and 164 kJ/mol, respectively, reported by Mintmire *et al.*[10] We compared the energies for two conformations with the ethyne hydrogens in a *trans* and *cis* conformation, respectively, about the ethyne carbon-carbon bond. The distal ethyne carbon in the *trans* and *cis* conformations was in an eclipsed and a staggered position, respectively, with respect to the subsurface carbons. An energy difference of only 7 kJ/mol was found. One can, however, note that the effects of basis-set superposition in most of these cases amount to as much as 77 kJ/mol (see Table V), introducing significant uncertainty into the precise values of the calculated adsorption energies. Since the methods used by both Pederson *et al.* and Mintmire *et al.* utilize similar Gaussian basis sets as the present study, or even smaller ones, the possible uncertainties due to BSSE should be kept in mind also when considering their LDA results.

## IV. CONCLUSION

The relative adsorption energies of different hydrocarbons ($CH_3\cdot$, $CH_2$, $CH\cdot$, $C_2H\cdot$, $C_2H_2$) and hydrogen, $H\cdot$, to a hydrogenated diamond (111) surface, were investigated by the *ab initio* molecular-orbital method. A major part of the work was a methodological study in which the effects of electron correlation corrections, template size, and basis set on the relative adsorption energies were investigated systematically. It was found that the template $C_{13}H_{21}\cdot$, containing six hydrogen neighbors to the dangling surface orbital, could be used successfully in modeling the hydrogenated (111) diamond surface. In the calculations, the gaseous and adsorbed species were completely geometry optimized, while it was shown to be sufficient to relax the central carbon atom in the template.

An electron correlation treatment, using the second-order Møller-Plesset model (MP2) resulted in the following order of the different species on the energy scale of adsorption:

$$C_2H\cdot > H\cdot \approx CH_2(\text{singlet}) > CH\cdot > CH_2\cdot(\text{triplet}) > CH_3\cdot > C_2H_2 \ .$$

This order of species was insensitive to which basis-set combination that was used in the calculations: 6-31$G^{**}$/STO-3$G$ or the more flexible 6-31$G^{**}$/6-31$G$, and also to corrections for basis-set superposition effects. Hence, the $C_2H\cdot$ and $CH_2$(singlet and triplet) species are predicted to adsorb much easier to the radical carbon atom on the diamond (111) surface than do $CH_3\cdot$ and

$C_2H_2$. The $C_2H_2$ species is, in fact, very weakly bound through its onefold site adsorption. However, the effect of the higher adsorption energies for $C_2H\cdot$ and $CH_2$ on the diamond growth is counteracted by the effect of the much lower gas-phase concentrations of these species during filament-assisted diamond deposition from a reaction mixture of methane and hydrogen. Kinetic modeling has shown that the concentrations of $CH_2$ and $C_2H\cdot$ are about two and four orders of magnitude, respectively, lower than the concentrations of $CH_3\cdot$ and $C_2H_2$, while the $C_2H_2$ concentration was estimated to be almost equal to the $CH_3\cdot$ concentration. We believe that these low concentrations especially preclude $C_2H\cdot$ from a significant role as a growth species. The significant difference in adsorption energy between $CH_3\cdot$ and $C_2H_2$, together with the fact that the gas-phase concentrations of these species are about the same, will then support a diamond growth mechanism based on the $CH_3\cdot$ group as a dominant growth species during filament-assisted deposition on the diamond (111) surface from a reaction mixture of methane and hydrogen. This result is consistent with earlier experimental results.

## ACKNOWLEDGMENTS

This work was supported by the Swedish Natural Science Research Council (NFR), the Swedish Research Council for Engineering Sciences (TFR), and the Angstrom consortium. The calculations were performed on the CRAY XMP/416 computer of the National Supercomputer Centre (NSC) in Linköping.

[1]M. Tsuda, M. Nakajima, and S. Oikawa, J. Am. Chem. Soc. **108**, 5780 (1986).
[2]M. Tsuda, M. Nakajima, and S. Oikawa, Jpn. J. Appl. Phys. **26**, L527 (1987).
[3]D. Huang, M. Frenklach, and M. Maroncelli, J. Phys. Chem. **92**, 6379 (1988).
[4]M. Frenklach and K. Spear, J. Mater. Res. **3**, 133 (1988).
[5]D. Huang and M. Frenklach, J. Phys. Chem. **95**, 3692 (1991).
[6]S. P. Mehandru and A. B. Andersson, J. Mater. Res. **5**, 2286 (1990).
[7]S. M. Valone, M. Trkula, and J. R. Laia, J. Mater. Res. **5**, 2296 (1990).
[8]M. R. Pederson, K. A. Jackson, and W. E. Picket, Phys. Rev. B **44**, 3891 (1991).
[9]M. R. Pederson, K. A. Jackson, and W. E. Picket, in *Proceedings of the 2nd International Conference on the New Diamond Science and Technology,* edited by R. Messier and J. Glass, MRS Symposia Proceedings No. 162 (Materials Research Society, Pittsburgh, 1991).
[10]J. W. Mintmire *et al.*, in *Proceedings of the 2nd International Conference on the New Diamond Science and Technology* (Ref. 9).
[11]W. D. Brenner, Phys. Rev. B **42**, 9458 (1990).
[12]M. J. Frisch *et al.*, GAUSSIAN90 (Gaussian Inc., Pittsburgh, PA, 1990).
[13]S. Veprek, J. Cryst. Growth **17**, 101 (1972).
[14]W. A. Lathan, W. J. Hehre, and J. A. Pople, J. Am. Chem. Soc. **93**, 808 (1971).
[15]S. F. Boys and F. Bernardi, Mol. Phys. **19**, 553 (1970); see also D. W. Schwenke and D. G. Truhlar, J. Chem. Phys. **82**, 2418 (1985).
[16]M. Page and D. W. Brenner, J. Am. Chem. Soc. **113**, 3270 (1991).
[17]K. A. Jackson, in *Proceedings of the 2nd International Conference on the New Diamond Science and Technology* (Ref. 9).
[18]W. J. Hehre *et al.*, *Ab Initio Molecular Theory* (Wiley, New York, 1986).
[19]C. J. Chu *et al.*, J. Appl. Phys. **70**, 1695 (1991).
[20]M. W. Geiss *et al.*, Appl. Phys. Lett. **58**, 2485 (1991).
[21]D. N. Belton and S. J. Harris, J. Chem. Phys. **96**, 2371 (1992).
[22]F. G. Celii *et al.*, Appl. Phys. Lett. **52**, 2043 (1988).
[23]S. J. Harris, A. M. Weiner, and T. A. Perry, Appl. Phys. Lett. **53**, 1605 (1988).
[24]S. J. Harris *et al.*, J. Appl. Phys. **66**, 5353 (1989).